Trans. Phenom. Nano Micro Scales, 8(2): 71-80, Summer and Autumn 2020
DOI: 10.22111/tpnms.2020.34038.1189

ORIGINAL RESEARCH PAPER

Crack fault detection in piezoelectric sensors using particle swarm optimization

Abbas Rahi[1,*], Reza Yarmohammadi[2]

[1]Assistant Professor, Faculty of Mechanical and Energy Engineering, Shahid Beheshti University, Tehran, Iran
[2]Ph.D. Candidate, Faculty of Mechanical and Energy Engineering, Shahid Beheshti University, Tehran, Iran

Received 20 April 2020; revised 8 October 2020; accepted 8 October 2020; available online 10 November 2020

ABSTRACT: Crack is one of the common types of defect in sensors that may cause system failure. In this paper, crack fault detection is considered in piezoelectric sensors. Piezoelectric sensors are assumed in micro-scale and cantilever-based MEMS sensors. Therefore, the usual methods used for macro-scale systems and FEMs to find natural frequencies cannot be used. To find the natural frequencies of the piezoelectric sensors, Modified Couple Stress Theory (MCST) and the Hamilton principle are used. Crack is modeled with a torsional spring whose stiffness depends on the depth and location of the cracks and the material length scale parameter. The PSO optimization algorithm is used to find the depth and location of the crack in the sensor. The results of optimization indicate the proper performance of the Particle Swarm Optimization (PSO) algorithm for detecting the crack in piezoelectric sensors. The results of the PSO algorithm are accurate for cracks near the fixed end of the sensor and are acceptable for cracks near the free end.

KEYWORDS: *Crack detection; MCST; Particle Swarm Optimization; piezoelectric sensor.*

INTRODUCTION

In recent decades, piezoelectric sensors are widely used in industries. These sensors are used in almost every application that needs to accurately measure or record dynamic variables such as pressure, force, and acceleration. The crack in piezoelectric sensors has a significant effect on their performance and may cause a failure in sensors. The cracks can change the dynamic behavior of the performance of the system, which can sometimes cause system failure. The presence of the crack reduces the natural frequency of the system, in other words, it increases displacement. Increasing displacement in piezoelectric sensors can cause sensor failure. The natural frequency in the sensors is very high due to their small scale, so the presence of cracks in the sensors causes a significant decrease in the natural frequency, which indicates the importance of crack study in the sensors [1-3].

Therefore, the natural frequency in the system can provide accurate information of the crack. Piezoelectric sensors have small dimensions on a micro scale. Normal frequencies in micro-sized systems cannot be calculated by the classical methods of continuous mechanics because of their small size. In recent years, several approaches such as Couple Stress Theory (CST) have been developed based on the effect of system size on its dynamic behavior [4-7].

The couple stress theory was proposed by Tiersten and Mindlin [8]. Yang et al. proposed the Modified Couple Stress Theory (MCST) to capture the size effect of the mechanical behaviors of microstructures using one constant of the mate-rial length scale parameter. Material length scale parameter is related to the material of the system and is a specified value for each material [9]. Today, there is a lot of research on the effect of size on the dynamic behavior of the systems with micro dimensions [10-16].

Also, several researches have been done to analyze the vibrations of a cracked beam in the macro-sized systems. Qian et al. [17] obtained the dynamic behavior and the stiffness matrix of the cracked beam. Orhan [18] analyzed the free and forced vibrations of a cantilever beam. Rios et al. [19] modeled the crack with a torsion spring to calculate the natural frequency of the cracked beam. Behzad et al. [20] obtained torsional spring stiffness for crack modeling for two different types of cracks. The mentioned studies have been done for macro-sized systems.

Tadi Beni et al. [21] and Loya et al. [22] analyzed the transverse vibrations of a cracked microbeam by modeling a torsion spring based on the MCST method. In microsystems, like the macro systems, the crack can be modeled with a torsion spring.

Recently, Rahi [23] evaluated the lateral vibration of cracked microbeam. He proposed four models for crack modeling with torsion spring. The torsional spring stiffness varied according to the location of the crack, the depth of the crack and material length scale parameter.

On the other hand, because the crack is one of the common defects in structures that can cause system failure, hence crack detection is important.

So, many studies have been conducted on crack detection in the last decade.

✉ *Corresponding Author Email: *a_rahi@sbu.ac.ir*
Tel.: +989372737526; Note. This manuscript was submitted on April 20, 2020; approved on October 8, 2020; published online November 10, 2020.

	Nomenclature		
A	cross section area (m^2)	$w(x,t)$	transverse deflection
E	Young's modulus		**Greek Symbols**
h	Thickness (μm)	ω	natural frequency (rad/s)
I	cross-section area-moment of inertia	ϑ	Poisson's ratio
L	length (μm)	π_s	strain energy
l	material length scale parameter	ρ	density (kg/m^3)
d	Depth of open-edge crack		**Subscripts**
K_t	Torsional spring coefficient	FEM	Finite Element Method
T	kinetic energy of the system	MCST	Modified Couple Stress Theory
t	Time (s)	MEMS	Micro-Electro-Mechanical-System
w	width (μm)	PSO	Particle Swarm Optimization
		CST	Couple Stress Theory

One of the most effective methods that has been dramatically improved is crack detection based on non-destructive testing.

In this method, the natural frequency of the system is compared with the natural frequency of the intact system, and it can be predicted whether or not there exists a crack. With the growth of science, researchers sought to identify the exact location and depth of the crack, using optimization methods.

Optimization methods are usually based on the population and the inspiration of the natural behavior of the beings in nature.

For optimal optimization, there should be enough information from the optimization problem, the optimization variables and the cost function.

If the crack detection in piezoelectric sensors is considered as an optimization problem, the depth and location of the crack are the optimization variables and the appropriate combination of the normal frequency of the intact system and the cracked system can be considered as the cost function [24].

A large number of studies have identified crack detection as an optimization problem. Shun and Rong [25] obtained the parameters of a crack in a macro beam with different boundary conditions with the genetically-simulated annealing hybrid algorithm.

Baghmisheh et al. [26] used a genetic algorithm to find the depth and location of the crack in a macro system. Moradi et al. [24] employed a bee optimization algorithm for crack detection in a macro beam.

Baghmisheh et al. [27] compared the accuracy of three optimization algorithms, PSO, Genetic, and neural networks to find the location and depth of the crack in a macro system. It was concluded that the PSO optimization algorithm has a more suitable function in determining the location and depth of the cracks than in the other two methods. Moezi et al. [28-30] identified the location and depth of the crack in the macro system by the cuckoo algorithm and the improvement of the cuckoo algorithm, also.

Erdogan [31] Identified the location and depth of cracks using linear and nonlinear properties of structural vibrations with hybrid optimization algorithm. Pitchaiah and Rao [32] identified the location and depth of cracks in thick beams based on information from the natural frequency of the system with neural networks.

As mentioned, a lot of research has been done on crack detection in macro structures.

In this study, crack fault detection is performed in piezoelectric sensors.

The crack is modeled with a torsional spring whose stiffness depends on the depth and location of the crack and the material length scale parameter.

Material length scale parameter depends on the characteristics of the material and can be experimentally obtained with several standardized tests.

The natural frequency of the piezoelectric sensor is obtained from the MCST approach and the Hamilton principle. With the PSO optimization method, the location and depth of the crack in the piezoelectric sensor are estimated.

The optimization results show the exact performance of the PSO optimization algorithm for detecting the crack near the fixed end of the piezoelectric cantilever-based MEMS sensor.

GEOMETRIC CHARACTERISTICS OF THE MICRO SENSOR WITH CRACK FAULT

The structural geometry of a piezoelectric cantilever based MEMS sensor along with the crack fault is shown in Figure 1.

The micro sensor consists of two layers. A silicon layer is located above the PZT with the length L and width W. In the actual sensor, both layers have the same thickness ($h_1 = h_2$) and h is total thickness ($h = h_1 + h_2$).

There is a straight open-edge crack of the depth d_c in the silicon layer.

This type of fault is usually due to fatigue [1]. For example, dimensions and mechanical properties of an actual sensor are mentioned in Table 1.

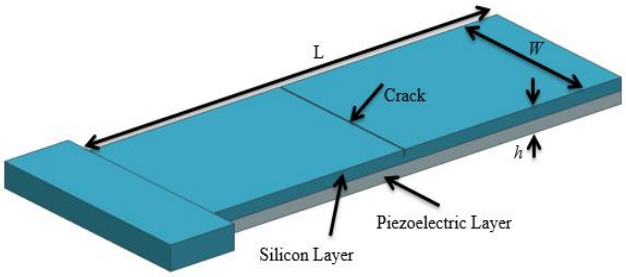


Fig. 1. Piezoelectric cantilever with an open-edge crack

Table1
Dimensions and mechanical properties of an actual sensor [1].

Symbol	Parameters	Values	Units
L	Length of PZT and Silicon	800	μm
W	Width of PZT and Silicon	300	μm
h_1	Thickness of Silicon	20	μm
ϑ_1	Poisson's ratio of Silicon	0.22	---
E_1	young's modulus of Silicon	170	GPa
ρ_1	Density of Silicon	2233	kg/m^3
h_2	Thickness of PZT	20	μm
ϑ_2	Poisson's ratio of Silicon	0.32	---
E_2	Young's modulus of PZT	63	GPa
ρ_2	Density of PZT	7550	kg/m^3
d_c	Depth of open-edge crack	1-10	μm

MODELLING OF A MEMS SENSOR WITH A CRACK

The piezoelectric cantilever-based sensor with a crack fault can be modeled as a cantilever beam as shown in Figure 2, where the crack is located at distance of L_c from the left support.

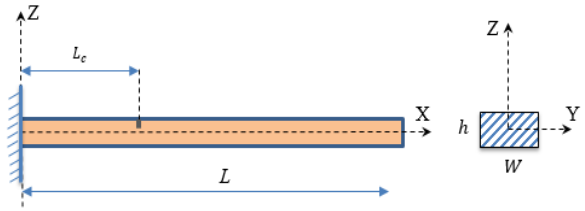


Fig. 2. Modeling of the cracked sensor

The piezoelectric cantilever consists of two layers that have different mechanical properties, for this reason, the equivalent mechanical properties can be calculated as follows [25]:

$$E = \frac{(E_2)^2\left(\frac{h_2}{h}\right)^4 + E_1^2\left(\frac{h_1}{h}\right)^4}{E_2\left(\frac{h_2}{h}\right) + E_1\left(\frac{h_1}{h}\right)} + \frac{2E_1E_2\left(\frac{h_2}{h}\right)\left(\frac{h_1}{h}\right)\left(2\left(\frac{h_2}{h}\right)^2 + 2\left(\frac{h_1}{h}\right)^2 + 3\left(\frac{h_2}{h}\right)\left(\frac{h_1}{h}\right)\right)}{E_2\left(\frac{h_2}{h}\right) + E_1\left(\frac{h_1}{h}\right)} \quad (1)$$

$$\rho = \frac{\rho_1 h_1 + \rho_2 h_2}{h_1 + h_2}$$
$$\vartheta = \frac{\vartheta_1 h_1 + \vartheta_2 h_2}{h_1 + h_2} \quad (2)$$
$$l = \frac{l_1 h_1 + l_2 h_2}{h_1 + h_2}$$

where E, I, ϑ, ρ and l are Young modulus, second moment of inertia, Poisson's ratio, density, and material length scale parameter, respectively.

To calculate the equation of motion of the cracked cantilever beam, it is divided into two uniform segments joined by torsion spring that is shown in Figure 3. The stiffness of torsion spring is calculated based on crack depth and geometrical and mechanical characteristics of the cantilever microbeam.

The torsional spring coefficient, K_t can be obtained as follows [21]:

$$K_t = \left[1 + \frac{6}{(1+\vartheta)\left(1-\frac{d_c}{h}\right)^2}\left(\frac{l}{h}\right)^2\right]^{-1} \left[\frac{36EI\left(1-\frac{d_c}{h}\right)^3}{25\pi h(1-\vartheta^2)\left(\frac{d_c}{h}\right)^2\left(3-\frac{d_c}{h}\right)}\right] \quad (3)$$

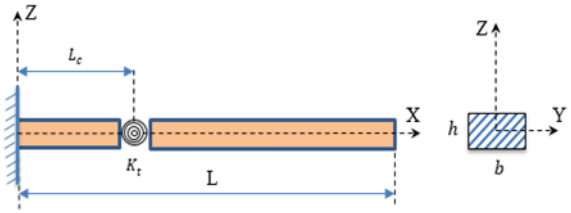


Fig. 3. Modeling open edge cracks with torsional springs

GOVERNING EQUATIONS

According to the previous section, the piezoelectric cantilever based MEMS sensor can be modeled with micro-beam.

The strain energy, π of each segment of the micro-beam based on the MCST can be obtained as follows [21, 28]:

$$\pi = \frac{1}{2}\int_0^L EI\left[1 + \frac{6}{1+\vartheta}\left(\frac{l}{h}\right)^2\right]\left(\frac{\partial^2 w}{\partial x^2}\right)^2 dx \quad (4)$$

If the $w_1(x,t)$ and $w_2(x,t)$ describe the displacement of the cantilever micro-beam segments at left and right sides of the torsional spring, respectively, the strain energy of the system can be obtained as follows:

$$\pi = \int_0^{L_c} \frac{1}{2} S \left(\frac{\partial^2 w_1}{\partial x^2}\right)^2 dx + \int_{L_c}^{L} \frac{1}{2} S \left(\frac{\partial^2 w_2}{\partial x^2}\right)^2 dx + \frac{1}{2} K_t \left(\frac{\partial w_2}{\partial x} - \frac{\partial w_1}{\partial x}\right)^2 \quad (5)$$

Also, the kinetic energies of the system can be written as follows:

$$T = \frac{1}{2}\int_0^{L_c} \rho A \left(\frac{\partial w_1}{\partial t}\right)^2 dx + \frac{1}{2}\int_{L_c}^{L} \rho A \left(\frac{\partial w_2}{\partial t}\right)^2 dx \quad (6)$$

Therefore, the governing equations of motion of the cantilever micro beam can be derived based on the MCST and Hamilton's principle as follows:

$$\begin{aligned} &\frac{\partial^2}{\partial x^2}\left(S\frac{\partial^2 w_1}{\partial x^2}\right) + \rho A \frac{\partial^2 w_1}{\partial t^2} = 0 \\ &\frac{\partial^2}{\partial x^2}\left(S\frac{\partial^2 w_2}{\partial x^2}\right) + \rho A \frac{\partial^2 w_2}{\partial t^2} = 0 \end{aligned} \quad (7)$$

where

$$S = EI\left[1 + \frac{6}{1+\vartheta}\left(\frac{l}{h}\right)^2\right] \quad (8)$$

The solution of governing equations 7 can be obtained as follows:

$$\begin{aligned} &w_i(x,t) = W_i(x)\,.\,T_i(t)\,; \quad i = 1,2 \\ &T_i(t) = A_i\, sin(\omega t) + B_i\, cos(\omega t) \end{aligned} \quad (9)$$

By substituting equation 9 into equations 7 and with some algebraic simplification, we have

$$\frac{d^4 W_i}{dx^4} - \beta^4 W_i(x) = 0 \quad ; \quad \beta^4 = \frac{\rho A \omega^2}{S} \quad (10)$$

where ω is natural frequency, ρ is the material density, and A is the cross-section of the microbeam.

The general solution of equation10 for the left and right segments of the torsional spring can also be derived as follows:

$$\begin{aligned} &W_1(x) = D_1 \cos(\beta x) + D_2 \sin(\beta x) + \\ &D_3 \cosh(\beta x) + D_4 \sinh(\beta x) \;\; ; \;\; 0 \le x \le L_c \end{aligned} \quad (11)$$

$$\begin{aligned} &W_2(x) = D_5 \cos(\beta x) + D_6 \sin(\beta x) + \\ &D_7 \cosh(\beta x) + D_8 \sinh(\beta x) \;\; ; \;\; L_c \le x \le L \end{aligned} \quad (12)$$

where $D_i\,, (i = 1, 2, \dots, 8)$ are constants, $W_1(x)$ and $W_2(x)$ are the equations of motion for the left and right segments of the crack, respectively.

The boundary conditions of the cracked cantilever beam can be expressed as follows:

$$\begin{aligned} &W_1(0) = 0 \;\; ; \;\; \frac{dW_1}{dx}(0) = 0 \\ &\frac{\partial^2 W_2}{\partial x^2}(L) = 0 \;\; ; \;\; \frac{\partial^3 W_2}{\partial x^3}(L) = 0 \\ &W_1(L_c) = W_2(L_c) \;\; ; \;\; \frac{\partial^2 W_1}{\partial x^2}(L_c) = \\ &\frac{\partial^2 W_2}{\partial x^2}(L_c) \;\; ; \;\; \frac{\partial^3 W_1}{\partial x^3}(L_c) = \frac{\partial^3 W_2}{\partial x^3}(L_c) \\ &\frac{\partial^2 W_1}{\partial x^2}(L_c) = \frac{K_t}{S}\left[\frac{\partial W_2(L_c)}{\partial x} - \frac{\partial W_1(L_c)}{\partial x}\right] \end{aligned} \quad (13)$$

By substituting equations 13 into equations 11 and 12, a set of 8 algebraic equations resulting in matrix form can be written as follows:

$$\begin{bmatrix} 1 & 0 & 1 & 0 & 0 & 0 & 0 & 0 \\ 0 & 1 & 0 & 1 & 0 & 0 & 0 & 0 \\ B_1 & B_2 & B_3 & B_4 & -B_1 & -B_2 & -B_3 & -B_4 \\ -B_1 & -B_2 & B_3 & B_4 & B_5 & B_6 & -B_7 & -B_8 \\ B_2 & -B_1 & B_4 & B_3 & -B_6 & B_5 & -B_8 & -B_7 \\ -B_1 - KB_2 & -B_2 + KB_1 & B_3 + KB_4 & B_4 + KB_3 & -KB_6 & KB_5 & KB_8 & KB_9 \\ 0 & 0 & 0 & 0 & -B_5 & -B_6 & B_7 & B_8 \\ 0 & 0 & 0 & 0 & B_6 & -B_5 & B_8 & B_7 \end{bmatrix} \times \begin{bmatrix} D_1 \\ D_2 \\ D_3 \\ D_4 \\ D_5 \\ D_6 \\ D_7 \\ D_8 \end{bmatrix} = 0 \quad (14)$$

where

$$\begin{aligned} &B_1 = \cos(\beta L_c)\,; B_2 = \sin(\beta L_c)\,; \\ &B_3 = \cosh(\beta L_c)\,; B_4 = \sinh(\beta L_c) \\ &B_5 = \cos(\beta L)\,; B_6 = \sin(\beta L)\;; \\ &B_7 = \cosh(\beta L)\,;\;\; B_8 = \sinh(\beta L)\;;\; K = \frac{K_t}{S\beta} \end{aligned} \quad (15)$$

The natural frequencies of the system can be calculated by zeroing the determinant of coefficient matrix in equation14.

VERIFICATION

In order to study the accuracy of ANSYS software in obtaining the natural frequencies of microbeams, five different beams with similar mechanical properties and dimensions appropriate to the model considered in this study are used**.** In ANSYS software, the number of elements in each of the five models is considered the same. The dimensions of these five different beams and the first natural frequency obtained from the analytical and the finite element solution have been presented in Table 2. As shown, with the smaller dimensions of the beam, the difference between the results of the finite element method and the analytical method increase significantly. This indicates the inadequacy of the finite element software in obtaining the micro-beams natural frequencies. Figure 4 shows the first natural frequency of the micro-beam in the ANSYS software. Therefore, the sensors due to their small dimensions cannot be modeled using the equations used for macro systems. In order to consider the effect of dimensions to calculate the natural frequencies of the system, the parameter l, which is dependent on the material of the system, is used. The equation of motion of the micro-cantilever sensors can be derived as follows:

$$EI\left[1+\frac{6}{1+\vartheta}\left(\frac{l}{h}\right)^2\right]\frac{\partial^4 w}{\partial x^4}+\rho A\ddot{w}=0 \qquad (16)$$

When the size of the system is large enough, $\frac{l}{h}\approx 0$, the equation of motion will be as follows:

$$EI\frac{\partial^4 w}{\partial x^4}+\rho A\ddot{w}=0 \qquad (17)$$

Equation 17 is the same as the classic form of the equation of motion of the cantilever beam.

Tab1e 2
Dimensions and their first natural frequency of the beam.

Model number	L (mm)	W (mm)	t (mm)	Analytical method (Hz)	FEM method (Hz)	Difference between FEM and Analytical methods
1	8000	3000	400	4.5207	4.5801	0.0594
2	800	300	40	45.2072	45.801	0.5938
3	80	30	4	452.0717	458.01	5.9383
4	8	3	0.4	4520.7168	4580.1	59.3832
5	0.8	0.3	0.04	45207.1684	45801	593.8316

To find the material length scale parameter of the piezoelectric sensors considered in this study, the effect of this parameter on the first natural frequency of the micro-sensor have been shown in Figure 5.

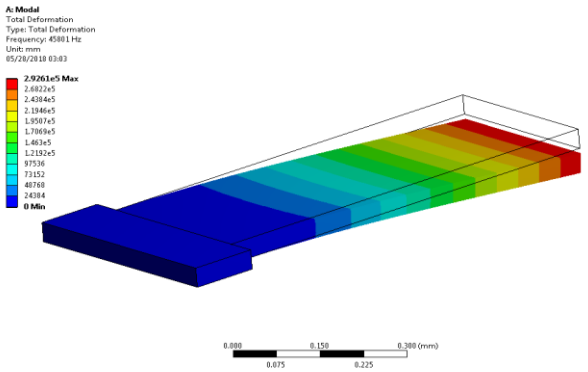


Fig. 4. The first natural frequency of the micro-beam in the ANSYS software

According to experimental result [1], the first natural frequency of this sensor is about 45430 Hz, which according to the results shown in Figure 5, the material length scale parameter for the piezoelectric MEMS sensor can be considered about 3.2 µm.

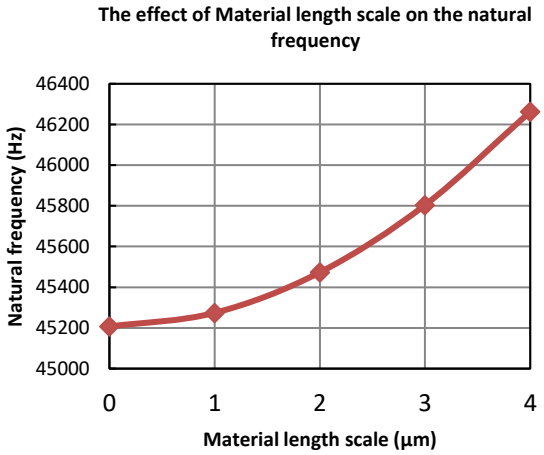


Fig. 5. Effect of material length scale parameter on the first natural frequency

Effects of location and depth of the crack on natural frequencies

In this section, the effects of location and depth of crack on natural frequencies are investigated. The first three natural frequencies and physical properties of the cantilever MEMS sensor without crack have been presented in Table 3. As shown in Figures 6 to 8, the presence of the crack reduces the natural frequencies of the beam. The reduction of the natural frequencies depends on the two parameters of the location and the depth of the crack.

As shown, if the crack is close to the fixed support of the cantilever MEMS sensor, with increasing crack depth, the first natural frequency will decrease significantly. The effects of changes in the location and the depth of the crack are prominent on higher frequencies.

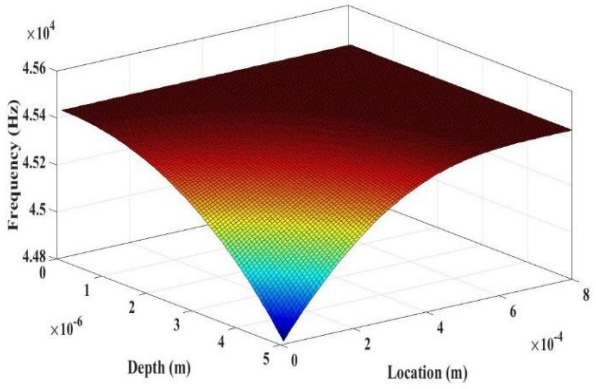


Fig. 6. The first natural frequency of Euler-Bernoulli cantilever MEMS sensor with respect to the location and depth of the crack

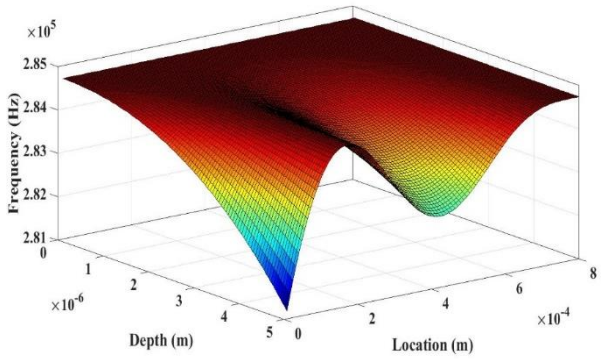


Fig. 7. The second natural frequency of Euler-Bernoulli cantilever MEMS sensor with respect to the location and depth of the crack

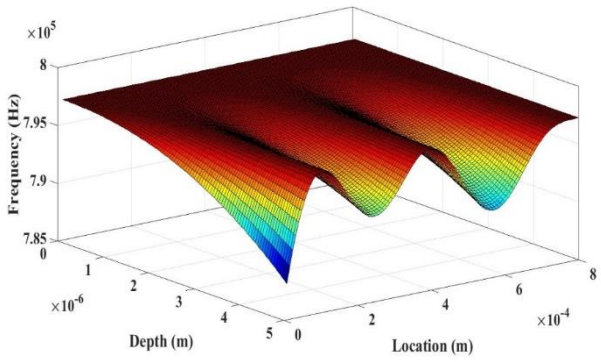


Fig. 8. The third natural frequency of Euler-Bernoulli cantilever MEMS sensor with respect to the location and depth of the crack

Table 3
The first three natural frequencies of the intact cantilever MEMS sensor.

$f_1\ (Hz)$	$f_2\ (Hz)$	$f_3\ (Hz)$
45430	284706	797184

$\vartheta = 0.27;\ E = 98.07\ GPa\ ;\ \rho = 4891.5\ kg/m^3\ ;$
$h = 40\ \mu m\ ;\ W = 300\ \mu m\ ;\ L = 800\ \mu m$

Crack fault detection in the MEMS sensor

The presence of cracks reduces the natural frequencies of the system. Reducing natural frequencies reduces the performance of piezoelectric sensors. For this reason, crack detection can have a significant effect on the performance of sensors. In order to identify the location and depth of the crack, the following optimization problem is used.

Minimize of

$$cost\ function\ (l_c, d_c) = \sum_{i=1}^{n} w_i \left(\frac{F_i^* - F_i}{f_i}\right)^2 \quad (18)$$

Subjected to:
$0 \le l_c \le L$
$0 \le d_c \le h$

where f_i, F_i, F_i^*, w_i, are ith natural frequency of the intact sensor, ith measured natural frequency of the cracked microbeam, ith natural frequency calculated by the optimization algorithm, ith weight factor, respectively. As shown in Figures 9 and 10, changes in natural frequencies by changing the location and depth of crack, increase at higher natural frequencies. To increase the effect of lower natural frequencies in the cost function, the weight factor for ith natural frequency is considered to be $\frac{1}{i}$ [27]. In this study, three natural frequencies for crack detection optimization were used. The purpose of optimization is to achieve the cost function at zero. In this study Particle Swarm Optimization (PSO) algorithm has been used for crack detection in micro-beam.

Changing the location and the depth of the crack will change the natural frequencies of the system. In order to investigate the changes of cost function corresponding to the change of crack location and depth, two different cracks according to Table 4 are considered. As shown in Figures 9 and 10, if the cracks reach the free end of the sensor, local minima of the cost function increase. For this reason, it is expected that it will be difficult for the optimization algorithm to find cracks at the end of the sensor.

Table 4
The results of the first three natural frequencies of the tests.

Test No.	Crack loc. (μm)	Crack dep. (μm)	$f_1\ (Hz)$	$f_2\ (Hz)$	$f_3\ (Hz)$
1	50.000	3.000	45268.474	284111.883	96302.590
2	720.000	1.000	45430.132	284704.799	97167.360

NUMERICAL AND COMPARATIVE DISCUSSION

Particle swarm optimization parameter

To find the cracks in the MEMS sensors, the particle swarm optimization algorithm has been used. Parameters for PSO optimization are given in Table 5. Optimization flowcharts by particle swarm method are presented in Figure 11.

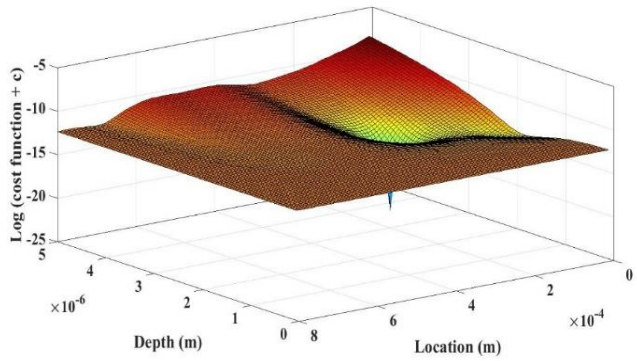


Fig. 9. Cost function variations for different location and depth of crack for test number 1

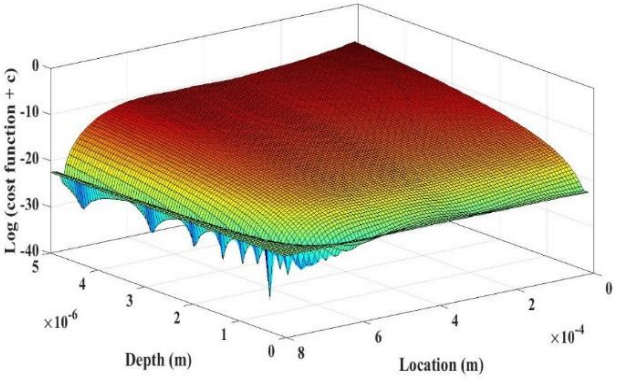


Fig. 10. Cost function variations for different location and depth of crack for test number 2

Table 5
Parameters of the PSO optimization algorithm.

Optimization method	Optimization parameter	Parameter value
PSO	Number of population	30
	Number of iteration	100
	w	0.5
	c_1	0.1
	c_2	0.9

RESULRS AND DISCUSSIONS

As described in the introduction, the crack may cause a failure in piezoelectric sensors, so detection of crack is important. In this section, 15 tests are used to assess the performance of the PSO optimization algorithm for finding the depth and location of the crack, which includes 5 different crack locations and 3 different crack depths. The geometric and mechanical properties of the piezoelectric sensor are considered in accordance with Table 1. Table 6 shows the first three natural frequencies for 15 tests. The PSO optimization algorithm has been used for detecting the desired cracks. Figure 12 shows the convergence of the PSO optimization algorithm for 4 samples. The objective function, after 100 iterations, is reduced to a decent ratio and approaches zero. The optimization results for 15 tests are presented in Table 7. With regard to the estimated results and the desired values, the percentage error of the PSO optimization algorithm can be obtained for each test as follows:

$$Error\% = \left|\frac{Estimation\ result - Desired\ value}{Desired\ value}\right| \times 100 \tag{18}$$

The error percentage of the PSO optimization algorithm shown in Table 8 illustrates the efficiency of this algorithm to quickly find the location and depth of the crack in piezoelectric sensors. Crack in piezoelectric sensors usually occurs near their fixed end [1-3]. The optimization results for the cracks that are closer to the fixed end are very accurate. As shown in Figures 9 and 10, if the cracks reach the free end of the sensor, local minima of the cost function increase. In the presence of cracks near the free end of the sensors, due to the low number of optimization iterations in this study, optimization results are acceptable. The maximum percentage error for crack location and depth is 1.984 and 19.867 percent, respectively.

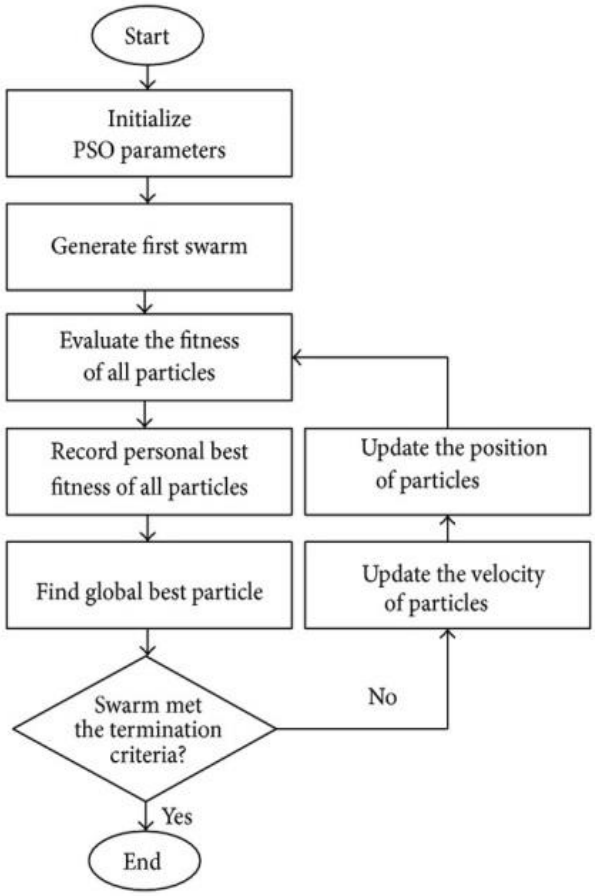


Fig. 11. Flowchart of the PSO algorithm

Table 6
Result for the first three natural frequencies for the 15 tests.

Test No.	Crack loc. (μm)	Crack dep. (μm)	f_2 (Hz)	f_2 (Hz)	f_3 (Hz)
1	50.000	1.000	45414.448	284647.917	797098.303
2	50.000	3.000	45268.474	284111.883	796302.590
3	50.000	5.000	44915.101	282833.498	794422.813
4	200.000	1.000	45422.010	284703.664	797073.081
5	200.000	3.000	45346.204	284683.669	796035.719
6	200.000	5.000	45161.285	284634.983	793520.067
7	400.000	1.000	45427.971	284645.855	797184.382
8	400.000	3.000	45407.725	284087.396	797183.192
9	400.000	5.000	45358.008	282730.743	797180.302
10	600.000	1.000	45429.959	284685.307	797011.491
11	600.000	3.000	45428.296	284493.624	795398.874
12	600.000	5.000	45424.203	284022.563	791474.356
13	750.000	1.000	45430.136	284705.632	797181.164
14	750.000	3.000	45430.128	284703.978	797149.802
15	750.000	5.000	45430.109	284699.908	797072.584

Table 7
The results of the estimation of location and depth of the crack.

Test No.	Desired value (μm)		Estimation results (μm)		Error %	
	Loc.	Dep.	Loc.	Dep.	Loc.	Dep.
1	50.000	1.000	50.000	1.000	0.000	0.000
2	50.000	3.000	50.000	3.000	0.000	0.000
3	50.000	5.000	50.000	5.000	0.000	0.000
4	200.000	1.000	200.000	1.000	0.000	0.000
5	200.000	3.000	200.000	3.000	0.000	0.000
6	200.000	5.000	200.000	5.000	0.000	0.000
7	400.000	1.000	400.000	1.000	0.000	0.000
8	400.000	3.000	400.000	3.000	0.000	0.000
9	400.000	5.000	400.000	5.000	0.000	0.000
10	600.000	1.000	599.999	1.000	0.000	0.000
11	600.000	3.000	600.000	3.000	0.000	0.000
12	600.000	5.000	600.000	5.000	0.000	0.000
13	750.000	1.000	742.851	1.156	0.953	15.600
14	750.000	3.000	740.212	3.596	1.305	19.867
15	750.000	5.000	764.877	5.294	1.984	5.880

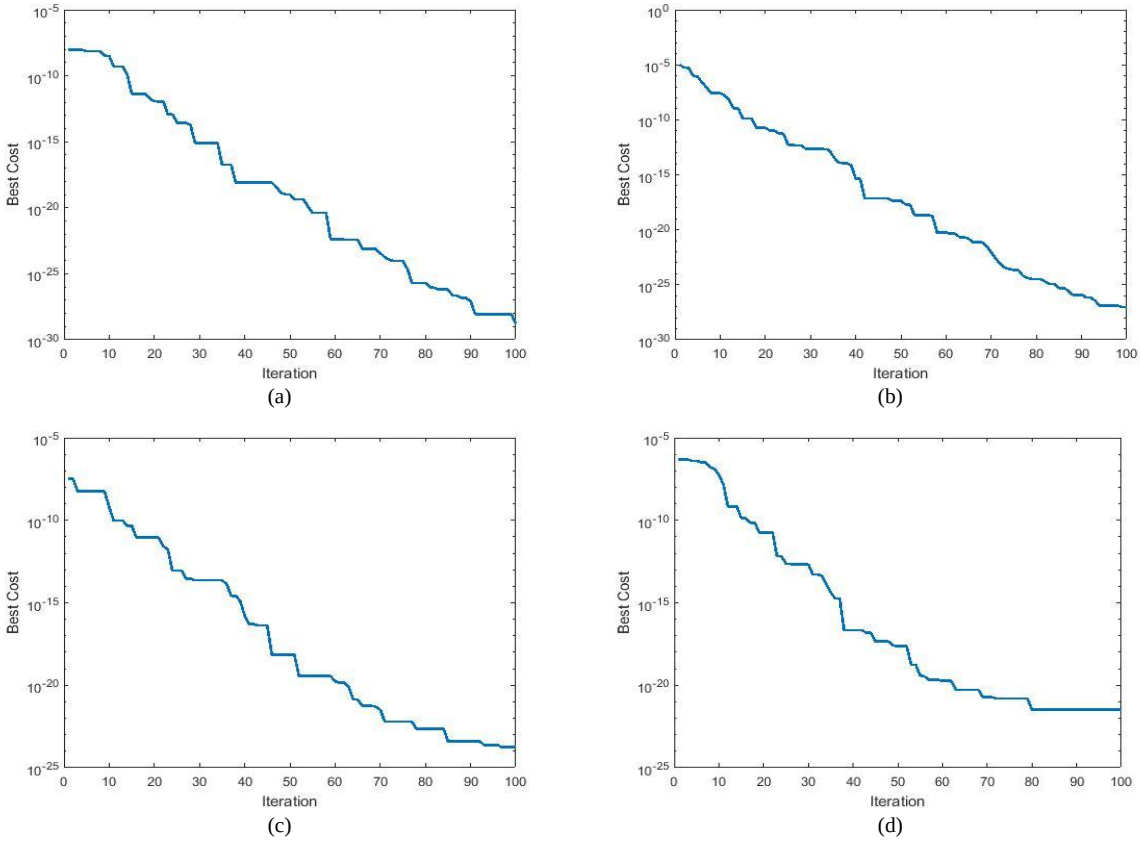


Fig. 12. The best value of the cost function at each iteration, a) Test 5, b) Test 6, c) Test 11, d) Test 12

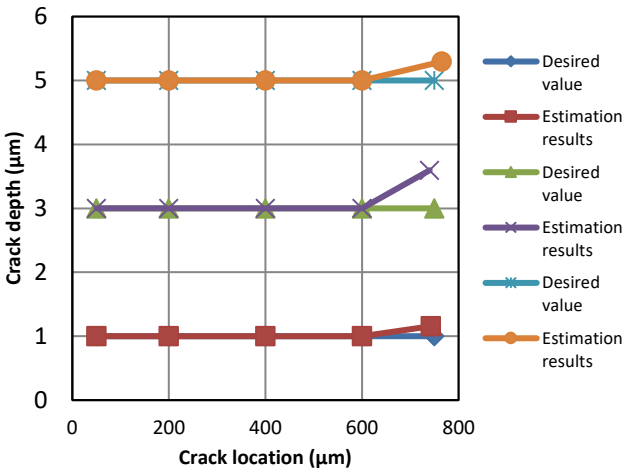


Fig. 13. The results of the estimation of location and depth of the crack

CONCLUSIONS

In this paper, crack fault detection was considered in piezoelectric sensors. The presence of the crack reduces the natural frequencies of the system. This decrease in the natural frequency in the sensors is more significant because of the micro-scale. For this reason, the crack investigation in piezoelectric sensors is very important. Common methods used to obtain natural frequencies in macro-scale systems cannot be used in micro-scale systems, and FEMs also do not provide acceptable results in these systems. The Modified Couple Stress Theory (MCST) and the Hamilton principle were used to find the natural frequencies of the piezoelectric sensors. The crack was modeled with a torsional spring whose stiffness depends on the depth and location of the cracks and the material length scale parameter. The PSO optimization algorithm was used to find the depth and location of the crack**.** In this study, 15 tests were used to assess the performance of the PSO optimization algorithm for finding the depth and location of the crack, which includes 5 different crack locations and 3 different crack depths Then, the percentage error of the PSO optimization algorithm was obtained. The optimization results show the exact performance of the PSO optimization algorithm for detecting a crack near the fixed end. If the crack is close to the free end of the sensor, due to the increase in the number of local minima of the cost function, the accuracy of the optimization algorithm is reduced. The maximum percentage error of the optimization algorithm for the location and depth of the cracks closest to the free-end sensor is 1.984 and 19.867 percent, respectively. Due to the low number of optimization iterations in this study, optimization results are acceptable.

REFERENCES

[1] Shoaib M, Hamid NH, Jan MT, Ali NB. Effects of crack faults on the dynamics of piezoelectric cantilever-based MEMS sensor. IEEE Sensors Journal. 2017 Aug 7;17(19):6279-94.

[2] Ho CM, Tai YC. Micro-electro-mechanical-systems (MEMS) and fluid flows. Annual review of fluid mechanics. 1998 Jan;30(1):579-612.

[3] Littrell R, Grosh K. Modeling and characterization of cantilever-based MEMS piezoelectric sensors and actuators. Journal of Microelectromechanical Systems. 2012 Jan 16;21(2):406-13.

[4] Lam DC, Yang F, Chong AC, Wang J, Tong P. Experiments and theory in strain gradient elasticity. Journal of the Mechanics and Physics of Solids. 2003 Aug 1;51(8):1477-508.

[5] Eringen AC. Nonlocal polar elastic continua. International journal of engineering science. 1972 Jan 1;10(1):1-6.

[6] Yang FA, Chong AC, Lam DC, Tong P. Couple stress based strain gradient theory for elasticity. International Journal of Solids and Structures. 2002 May 1;39(10):2731-43.

[7] Gurtin ME, ME G, AI M. Surface stress in solids. 1978:14(6): 431-440

[8] Mindlin RD, Tiersten HF. Effects of couple-stresses in linear elasticity. COLUMBIA UNIV NEW YORK; 1962 Jul.

[9] Kong S, Zhou S, Nie Z, Wang K. The size-dependent natural frequency of Bernoulli–Euler micro-beams. International Journal of Engineering Science. 2008 May 1;46(5):427-37.

[10] Akbaş ŞD. Free vibration of edge cracked functionally graded microscale beams based on the modified couple stress theory. International Journal of Structural Stability and Dynamics. 2017 Apr 31;17(03):1750033.

[11] Askari AR, Tahani M. Size-dependent dynamic pull-in analysis of geometric non-linear micro-plates based on the modified couple stress theory. Physica E: Low-dimensional Systems and Nanostructures. 2017 Feb 1;86:262-74.

[12] Alinaghizadeh F, Shariati M, Fish J. Bending analysis of size-dependent functionally graded annular sector microplates based on the modified couple stress theory. Applied Mathematical Modelling. 2017 Apr 1;44:540-56.

[13] Guo J, Chen J, Pan E. Free vibration of three-dimensional anisotropic layered composite nanoplates based on modified couple-stress theory. Physica E: Low-dimensional Systems and Nanostructures. 2017 Mar 1;87:98-106.

[14] He D, Yang W, Chen W. A size-dependent composite laminated skew plate model based on a new modified couple stress theory. acta mechanica solida sinica. 2017 Feb 1;30(1):75-86.

[15] Rahi A. Vibration analysis of multiple-layer microbeams based on the modified couple stress theory: analytical approach. Archive of Applied Mechanics. 2020 Sep 28:1-0.

[16] Rahi A. Analytical Approach for Vibration Analysis of a Microsensor with Two layers of Silicon and Piezoelectric based on MCST. Transp Phenom Nano Micro Scales. 2020 Feb 1;8(1):1-8.
[17] Qian GL, Gu SN, Jiang JS. The dynamic behaviour and crack detection of a beam with a crack. Journal of sound and vibration. 1990 Apr 22;138(2):233-43.
[18] Orhan S. Analysis of free and forced vibration of a cracked cantilever beam. Ndt & E International. 2007 Sep 1;40(6):443-50.
[19] Rizos PF, Aspragathos N, Dimarogonas AD. Identification of crack location and magnitude in a cantilever beam from the vibration modes. Journal of sound and vibration. 1990 May 8;138(3):381-8.
[20] Behzad M, Ghadami A, Maghsoodi A, Hale JM. Vibration based algorithm for crack detection in cantilever beam containing two different types of cracks. Journal of Sound and Vibration. 2013 Nov 25;332(24):6312-20.
[21] Jafari A. Size effect on free transverse vibration of cracked nano-beams using couple stress theory. International Journal of Engineering. 2015 Feb 1;28(2):296-304.
[22] Loya J, López-Puente J, Zaera R, Fernández-Sáez J. Free transverse vibrations of cracked nanobeams using a nonlocal elasticity model. Journal of applied physics. 2009 Feb 15;105(4):044309.
[23] Rahi A. Crack mathematical modeling to study the vibration analysis of cracked micro beams based on the MCST. Microsystem Technologies. 2018 Jul 1;24(7):3201-15.
[24] Moradi S, Razi P, Fatahi L. On the application of bees algorithm to the problem of crack detection of beam-type structures. Computers & Structures. 2011 Dec 1;89(23-24):2169-75.
[25] Hwang SF, He RS. Improving real-parameter genetic algorithm with simulated annealing for engineering problems. Advances in Engineering Software. 2006 Jun 1;37(6):406-18.
[26] Vakil-Baghmisheh MT, Peimani M, Sadeghi MH, Ettefagh MM. Crack detection in beam-like structures using genetic algorithms. Applied soft computing. 2008 Mar 1;8(2):1150-60.
[27] Baghmisheh MV, Peimani M, Sadeghi MH, Ettefagh MM, Tabrizi AF. A hybrid particle swarm–Nelder–Mead optimization method for crack detection in cantilever beams. Applied Soft Computing. 2012 Aug 1;12(8):2217-26.
[28] Moezi SA, Zakeri E, Zare A, Nedaei M. On the application of modified cuckoo optimization algorithm to the crack detection problem of cantilever Euler–Bernoulli beam. Computers & Structures. 2015 Sep 1;157:42-50.
[29] Moezi SA, Zakeri E, Zare A. A generally modified cuckoo optimization algorithm for crack detection in cantilever Euler-Bernoulli beams. Precision Engineering. 2018 Apr 1;52:227-41.
[30] Moezi SA, Zakeri E, Zare A. Structural single and multiple crack detection in cantilever beams using a hybrid Cuckoo-Nelder-Mead optimization method. Mechanical Systems and Signal Processing. 2018 Jan 15;99:805-31.
[31] Erdogan YS. A study on the crack detection in beams using linear and nonlinear normal modes. Advances in Structural Engineering. 2020 May;23(7):1305-21.
[32] Pitchaiah D, Rao PS. Optimized Deep Learning With Opposition-Based Ant Lion Approach For Crack Identification Of Thick Beams. Surface Review and Letters (SRL). 2020;27(08):1-0.